

# A Systematic Approach to Identify the Breast Cancer Grades in Histopathological Images Using Deep Neural Networks

S.H.S. Silva (1<sup>st</sup> Author)  
Department of Computer Science  
University of Sri Jayewardenepura  
Gangodawila, 10250, Sri Lanka  
hasinisandunika.usjp@gmail.com

T. M. K. K. Jinesena (2<sup>nd</sup> Author)  
Department of Computer Science  
University of Sri Jayewardenepura  
Gangodawila, 10250, Sri Lanka  
kasun@sjp.ac.lk

**Abstract** — Breast cancer can be recognized as one of the most well-known and life-threatening cancers impacting women and this has been identified as the second most common cancer across the world. According to registered data, there were over 2 million newly reported cases in 2020. The Deep Convolutional Neural Network has been identified as one of the most dominant and powerful deep learning approaches involved in the analysis of visual imagination. There are many shreds of evidence that indicate the appropriateness of this in medical imaging including breast cancer detection, classification, and segmentation with higher accuracy rates. The main intent of the research is to develop an automated application that can determine the Nottingham Histologic Score of a given input histopathological image obtained from breast cancer or healthy tissues with DenseNet based architecture. Healthy or benign tissues are categorized as zero and cancerous tissues are categorized based on the grade obtained as one, two, or three. In this study, we were able to obtain more than 94% accuracy rates for each trained model including 2-predict, 3-predict, and 4-predict networks. Further, a desktop-based inference tool that allows us to perform breast cancer grading was also developed as a result of this study.

**Keywords** — Breast Cancer Grading, Computer-Aided Diagnosis, DenseNet, Histopathological Images, Nottingham Histologic Score

## I. INTRODUCTION

Breast cancer is identified as the second most common cancer and this holds the highest mortality rate due to cancers among women worldwide. As per the Union for International Cancer Control organization, 2.3 million new cases were reported in 2020 [34]. Once the breast cancer cells are formed, that will lead to the spread of malignant cells to other parts of the body by making it life-threatening. Breast cancers are often found earlier when they are small and before they spread. Due to technical advancement, early detection, and procedures, the survival rate of breast cancer patients has significantly improved across the world within the last few years. Breast cancer grade classification is a labor-intensive

task and needs human experts and time to do the diagnoses. The grade of breast cancer tissue is calculated according to the way that cancer cells look under the microscope. For the laboratory breast cancer grade analysis purpose, it is best known that specimens of the tissues with the affected areas are used. Histopathological images are extracted as a result of this. It is known that histopathological images can be extracted with different High-Power Field (HPF) values. But images with 40X HPF values are well defined and illustrate the key features. The classified grade is used to figure out what treatments work best.

Densely Connected Convolutional Network (DenseNet) is one of the discoveries in deep neural networks for visual object recognition. Deep Convolutional Neural Networks (DCNN) with DenseNet architecture can be identified as one of the most dominant and powerful deep learning approaches involved in the analysis of visual imagination that provide excellent performance in medical imaging including breast cancer detection, classification, and segmentation with higher accuracy rates of more than 90% [32] [33]. This research aims to introduce a new computer-aided diagnosis approach that can continue the existing laboratory grading procedure with a higher accuracy rate.

## II. OBJECTIVES

Current study intends to develop an application that can determine the grade of a given histopathological image of breast cancer or healthy tissue as 0-benign, 1, 2, or 3 using a DenseNet based DCNN.

## III. METHODOLOGY

Below mentioned are the major tasks that had to be carried out during our research work.

- Data preprocessing

To complete the data preprocessing task, several mechanisms had to be applied and they are discussed under data preprocessing.

- Model building and evaluation

After completing the dataset preparation, built three DCNN models with DenseNet architecture as,

- ❖ 2-predict: classifies benign-0 and malignant-1

- ❖ 3-predict: classifies grades into grade 1, grade 2, and grade 3
- ❖ 4-predict: classifies as 0-benign, grade 1, grade 2, and grade 3.
- Implementation of the inference tool

To visualize the results obtained as well as to make the models available for use, an inference tool was built.

### A. Data Preprocessing

Initially, we received a graded (1, 2, and 3) dataset [11] with different HPF values (4X, 10X, 20X, 40X), resolutions, and image formats. To complete the data preprocessing task, we used a subset of the initial image dataset with 40X HPF value and increased that by applying several data augmentation techniques including image cropping, rotating, etc. Later we were able to create NumPy arrays for each grade with dimensions  $700*128*128*3$ .

Again, we have used another dataset [14] to train the 2-predict model and after applying preprocessing techniques on the received benign 40X HPF dataset, we have created a NumPy array for that with dimensions  $700*128*128*3$ . Fig. 1. illustrates an application of image augmentation by recreating images with cropping and rotating.

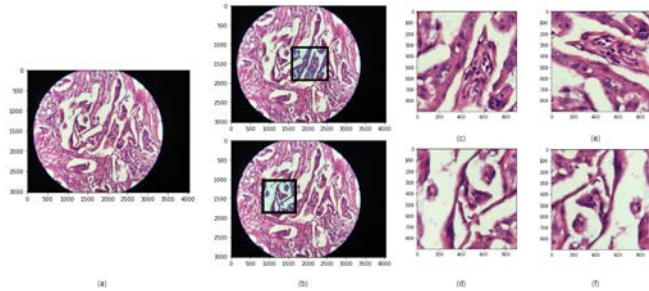


Fig. 1. Illustrates an application of Image Augmentation-(a) Original image, (b) Sub images to be extracted, (c,d) Extracted images, (e) Application of rotation up to 90 degrees for c, (f) Application of rotation up to 180 degrees for d.

For the 2-predict model implementation, the malignant dataset was created by applying the simple random sampling technique on the dataset of the 3-predict model. Dataset of the 4-predict model was created by combining both the benign image dataset of the 2-predict model and the dataset of the 3-predict model. Table 1. defines the dimensions of the training and testing datasets used in each model.

Table 1. Tabular Representation of the Datasets.

Model	Training Dataset	Testing Dataset
2-predict	600*128*128*3 for 0 600*128*128*3 for 1	100*128*128*3 for 0 100*128*128*3 for 1
3-predict	600*128*128*3 for 1 600*128*128*3 for 2 600*128*128*3 for 3	100*128*128*3 for 1 100*128*128*3 for 2 100*128*128*3 for 3
4-predict	600*128*128*3 for 0 600*128*128*3 for 1 600*128*128*3 for 2 600*128*128*3 for 3	100*128*128*3 for 0 100*128*128*3 for 1 100*128*128*3 for 2 100*128*128*3 for 3

### B. Model Building and Evaluation

To build each model, the following key aspects were considered; Grade classification was carried out by considering two scenarios. In the first scenario, a single neural network model was implemented to classify the histopathological images as benign-0, grade 1, grade 2, and grade 3. In the second scenario, two deep neural network models were trained to achieve the same objective as in the first scenario whereas implementing the initial model to classify the histopathological image as benign or malignant and at the second step, to classify the grade based on the prediction obtained at the first step. As in Fig. 2., the initial model classifies the input histopathological image as benign-0 or malignant-1 and if it is malignant, obtains the prediction from the second model as 1, 2, or 3 otherwise the grade will be remaining as zero.

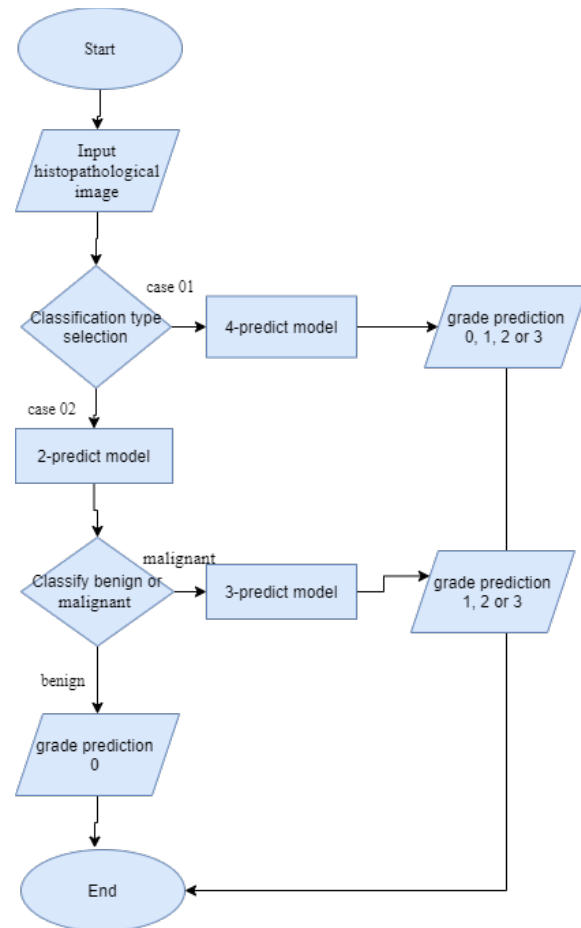


Fig. 2. Logical Overview of the Proposed Solution.

As per the research objectives that were mentioned in previous sections, this research is targeted at building a DCNN with transfer learning to predict the grades (0-benign, 1, 2, and 3) of histopathological images. Below define the architectures of transfer learning models, and the process of the evaluation carried out to achieve the above-defined goal.

### 1. Model Building

The transfer learning technique was applied to implement 2-predict, 3-predict, and 4-predict models for 128\*128 RGB image datasets, and we were able to receive better test accuracy rates. This model is a composition of,

- Pre-trained DenseNet-201 weights
- 2D global average pooling layer
- Dropout layer with 0.5 probability
- Batch normalization layer
- Densely connected layer with softmax operation

The following Fig. 3. illustrates the architecture of the transfer learning model. This was implemented with Spyder and Anaconda framework and the libraries, dependencies used were TensorFlow, Keras, sklearn, and OpenCV.

Layer (type)	Output Shape	Param #
densenet201 (Functional)	(None, 4, 4, 1920)	18321984
global_average_pooling2d (Gl	(None, 1920)	0
dropout (Dropout)	(None, 1920)	0
batch_normalization (BatchNo	(None, 1920)	7680
dense (Dense)	(None, 2)	3842
-----		
Total params:	18,333,506	
Trainable params:	18,100,610	
Non-trainable params:	232,896	

Fig. 3. The Architecture of the Transfer Learning Model.

Apart from that, a Flask Application Program Interface with Anaconda framework was developed to obtain the prediction by considering each case.

### 2. Evaluation

This was performed on the reserved test datasets of each model. For each model, there were around 14% of allocated histopathological images for testing purposes out of all images.

The evaluation was carried out by changing parameters including batch size, dropout probability, and the number of epochs. But, all three models provided significant responses only for the varied number of epochs rather than batch size and dropout probability. Mainly we have performed evaluation operations on test datasets including test accuracy rate calculation, confusion matrix illustration, and classification reports.

### C. Implementation of the Inference Tool

This was carried out to visualize the results obtained and to make the trained models available for use. The inference tool was implemented as a desktop graphical user interface application and has added some basic graphical user interface functions such as uploading an image, viewing results, saving an image with the classification, searching a record by ID, deleting a record by ID, converting a record into PDF format with a suitable database connection.

The summarized architecture of the proposed solution is illustrated in Fig. 4.

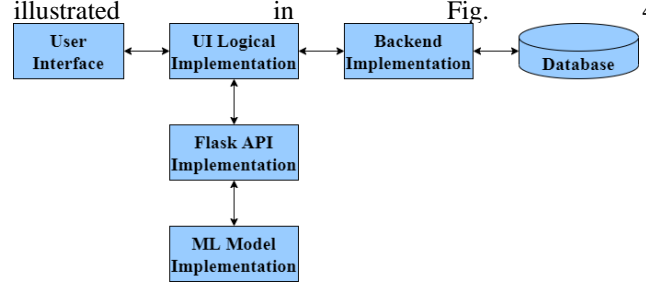


Fig.4. Summarized Architecture of the Proposed Solution.

This was implemented with Apache NetBeans with Maven dependencies and MongoDB was used as the database.

Apart from that, an Application Program Interface integration was carried out to obtain the predictions by considering each case as 1 and 2.

## IV. RESULTS AND DISCUSSION

To analyze the results generated by each model, the main method that followed was the test data-based results generation. The following includes the results obtained and the comparison between the obtained results.

### A. Two-Predict Model

Fig. 5. shows the loss vs epochs received by applying transfer learning during the process of training for the two-predict model with 20 epochs. As per this, curves of both validation and training are getting converged with the number of epochs. We could see that the model attains to the minimum loss rate at around the 4<sup>th</sup> epoch and continues the same until the 20th epoch. This indicates that the model shows a good fit with the training dataset.

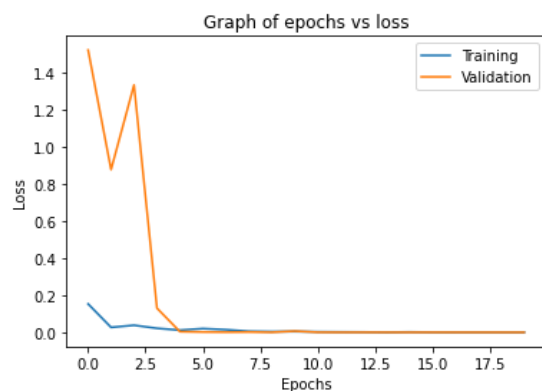


Fig. 5. Loss vs Epochs for Two-Predict Model.

Fig. 6. shows the normalized confusion matrix received by applying transfer learning from the testing dataset for the two-predict model with 20 epochs.

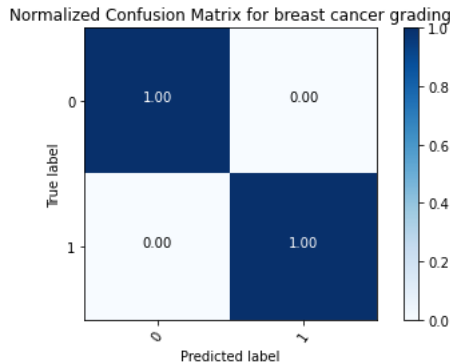


Fig. 6. Normalized Confusion Matrix for Two-Predict Model.

Fig. 7. shows the classification report received by applying transfer learning from the testing dataset for the two-predict model with 20 epochs. According to this result, precision, recall, and F1-score have obtained the highest values as can be obtained. Also, the accuracy received for the test dataset is 100%.

```

In [13]: print(classification_report( true_y.argmax(axis=-1), y_predict))
          precision    recall  f1-score   support

   0       1.00      1.00      1.00      100
   1       1.00      1.00      1.00      100

 accuracy          1.00      1.00      1.00      200
 macro avg          1.00      1.00      1.00      200
 weighted avg          1.00      1.00      1.00      200
    
```

Fig. 7. Classification Report for Two-Predict Model.

### B. Three-Predict Model

Fig. 8. shows the loss vs epochs received by applying transfer learning during the process of training for the three-predict model with 30 epochs. This model was previously trained for 20 epochs. As per that, the trained model with 30 epochs tends to converge with the number of epochs rather than the model with 20 epochs. This indicates that the model with 30 epochs shows a better fit with the training dataset than the model with 20 epochs.

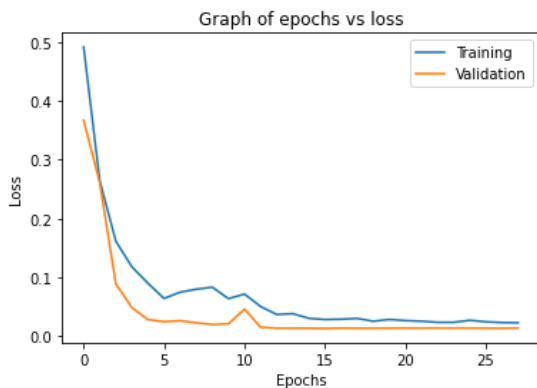


Fig. 8. Loss vs Epochs for Three-Predict Model.

Fig. 9. shows the normalized confusion matrix received by applying transfer learning from the testing dataset for the three-predict model with 30 epochs.

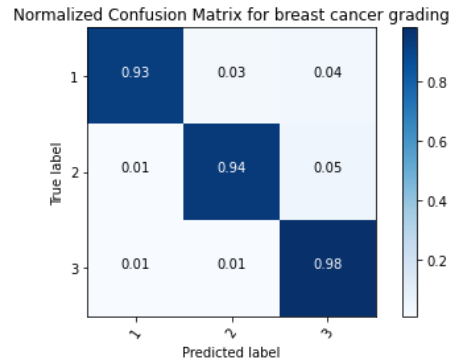


Fig. 9. Normalized Confusion Matrix for Three-Predict Model.

Fig. 10. shows the classification report received by applying transfer learning from the testing dataset for the three-predict model with 30 epochs. As this was trained for 20 epochs previously, the trained model with 30 epochs holds maximum values for precision, recall, and F1-score. The test accuracy rates of trained models with 20 and 30 epochs are 94.33% and 94.99% respectively.

```

In [47]: print(classification_report( true_y.argmax(axis=-1), y_predict))
          precision    recall  f1-score   support

   0       0.98      0.93      0.95      100
   1       0.96      0.94      0.95      100
   2       0.92      0.98      0.95      100

 accuracy          0.95      0.95      0.95      300
 macro avg          0.95      0.95      0.95      300
 weighted avg          0.95      0.95      0.95      300
    
```

Fig. 10. Classification Report for Three-Predict Model.

### C. Four-Predict Model

Fig. 11. shows the loss vs epochs received by applying transfer learning during the process of training for the four-predict model with 25 epochs. As this was previously trained for 20 and 30 epochs, the trained model with 25 epochs shows much convergence between validation and training curves. This indicates that the model with 25 epochs shows a good fit with the training dataset.

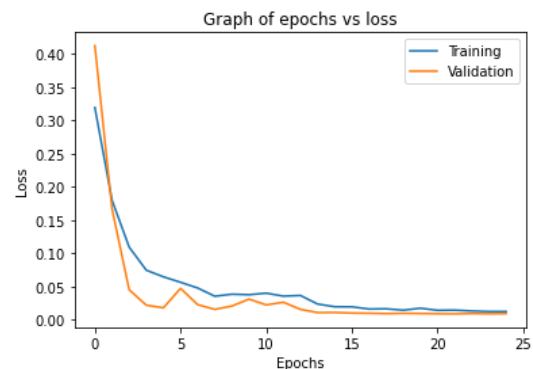


Fig. 11. Loss vs Epochs for Four-Predict Model.

Fig. 12. shows the normalized confusion matrix received by applying transfer learning from the testing dataset for the four-predict model with 25 epochs.

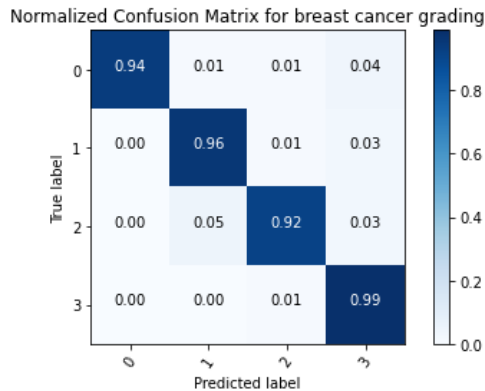


Fig. 12. Normalized Confusion Matrix for Four-Predict Model.

Fig. 13. show the classification report received by applying transfer learning from the testing dataset for the four-predict model with 25 epochs. As per previous results for 20 and 30 epochs, the trained model with 25 epochs holds maximum values for precision, recall, and F1-score. The test accuracy rates of trained models with 20, 25, and 30 epochs are 92.75%, 95.2499%, and 94.7499% respectively.

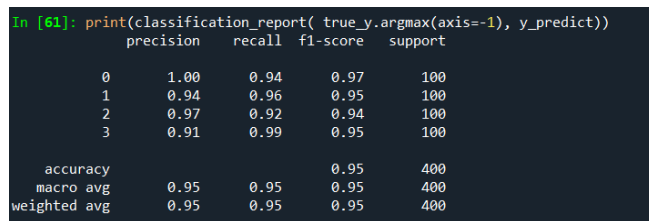


Fig. 13. Classification Report for Four-Predict Model.

#### D. Model Type (Case 1 and 2)

Fig. 14. shows the test accuracy rates received by performing case 1 and 2 operations for the test dataset of the 4-predict model. This was implemented with the 2-predict model with 20 epochs, the 3-predict model with 30 epochs, and the 4-predict model with 25 epochs.

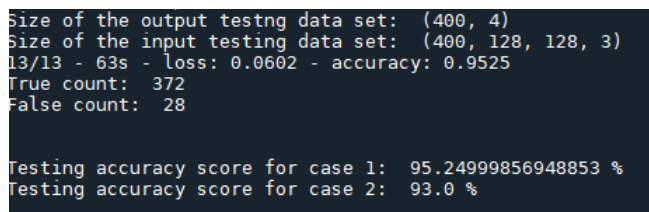


Fig. 14. Test Accuracy Rates of Case 1 and 2.

According to the results obtained,

- Two-predict model: When Fig. 5 is considered, we could see that the graph is getting converged whereas increasing the number of epochs. Fig. 6 and 7 also evidently express the appropriateness of the model by providing a 100% accuracy rate for the test dataset.
- Three-predict model: When Fig. 8 is considered, we could see that we can obtain a good fit by increasing the number of epochs up to 30. Fig. 9 and 10 also provide some evidence, providing a 94.99% accuracy rate for the test dataset for 30 epochs.

- Four-predict model: By considering Fig. 11, we can conclude that we can increase the fitness of the model by increasing the number of epochs up to 25. Fig. 12 and 13 also show a higher test data accuracy rate around 95.249% for 25 epochs.

- Model type (case 1 and 2) comparison: According to Fig. 14, can conclude that both approaches are good enough, and also both are applicable for the desktop graphical user interface prediction purpose.

By referring to the above results, we can conclude that it is appropriate to train the two-predict model up to 20 epochs, the three-predict model up to 30 epochs, and the four-predict model up to 25 epochs. Furthermore, both model types (case 1 and 2) are applicable for the desktop graphical user interface prediction purpose.

## V. CONCLUSION

In this research, three DCNN based models with transfer learning have been implemented to classify the grades of breast cancer. These DCNN models have been trained and tested with histopathological image datasets with the 40X HPF value. 2-predict, 3-predict, and 4-predicts models were able to obtain test accuracy rates of 100%, 94.999%, and 95.2499% respectively. Further, this research confirms the successfulness of using transfer learning with DenseNet architecture whereas providing test accuracy rates of more than 94% for all three trained models. Moreover, a desktop application was developed to infer the solution. Ultimately, accuracy improvements, implementation of the developed system as a web-based application could be identified as work that could be carried out as further improvements of this research.

## REFERENCES

- [1] T. Mahmood, M. Arsalan, M. Owais, M. B. Lee, and K. R. Park, "Artificial intelligence-based mitosis detection in breast cancer histopathology images using Faster R-CNN and deep CNNs," *J. Clin. Med.*, vol. 9, no. 3, p. 749, 2020.
- [2] D. C. Cireşan, A. Giusti, L. M. Gambardella, and J. Schmidhuber, "Mitosis detection in breast cancer histology images with deep neural networks," *Med. Image Comput. Comput. Assist. Interv.*, vol. 16, no. Pt 2, pp. 411–418, 2013.
- [3] T. Mahmood, S. Ziauddin, A. R. Shahid, and A. Safi, "Mitosis detection in breast cancer histopathology images using statistical, color and shape-based features," *J. Med. Imaging Health Inform.*, vol. 8, no. 5, pp. 932–938, 2018.
- [4] M. A. Aswathy and M. Jagannath, "Detection of breast cancer on digital histopathology images: Present status and future possibilities," *Inform. Med. Unlocked*, vol. 8, pp. 74–79, 2017.
- [5] A. Tashk, M. S. Helfroush, H. Danyali, and M. Akbarzadeh-jahromi, "Automatic detection of breast cancer mitotic cells based on the combination of textural, statistical and innovative mathematical features," *Appl. Math. Model.*, vol. 39, no. 20, pp. 6165–6182, 2015.
- [6] H. Wang et al., "Mitosis detection in breast cancer pathology images by combining handcrafted and convolutional neural network features," *J. Med. Imaging (Bellingham)*, vol. 1, no. 3, p. 034003, 2014.
- [7] T. X. Jian, M. Nazahah, M. M. Yusoff, and A. R. K. Shakir, "Mitotic cell detection in breast histopathology image: A review," *J. Phys. Conf. Ser.*, vol. 1372, p. 012026, 2019.
- [8] S. Rao, "Mitosis-RCNN: Mitotic figure detection in breast cancer histopathology images using region-based convolutional neural networks," 2018.

- [9] T. K. ten Kate, J. A. Beliën, A. W. Smeulders, and J. P. Baak, "Method for counting mitoses by image processing in Feulgen stained breast cancer sections," *Cytometry*, vol. 14, no. 3, pp. 241–250, 1993.
- [10] M. Veta et al., "Assessment of algorithms for mitosis detection in breast cancer histopathology images," *Med. Image Anal.*, vol. 20, no. 1, pp. 237–248, 2015.
- [11] H. Bolhasani, E. Amjadi, M. Tabatabaieian, and S. J. Jassbi, "A histopathological image dataset for grading breast invasive ductal carcinomas," *Inform. Med. Unlocked*, vol. 19, no. 100341, p. 100341, 2020.
- [12] "Staging & Grade," *Jhu.edu*. [Online]. Available: <https://pathology.jhu.edu/breast/staging-grade/>. [Accessed: 12-Jun-2021].
- [13] F. A. Spanhol, L. S. Oliveira, C. Petitjean, and L. Heutte, "Breast cancer histopathological image classification using Convolutional Neural Networks," in *2016 International Joint Conference on Neural Networks (IJCNN)*, 2016.
- [14] F. A. Spanhol, L. S. Oliveira, C. Petitjean, and L. Heutte, "A Dataset for Breast Cancer Histopathological Image Classification," *IEEE Trans. Biomed. Eng.*, vol. 63, no. 7, pp. 1455–1462, 2016.
- [15] A. Fernando, U. Jayarajah, S. Prabashani, E. A. Fernando, and S. A. Seneviratne, "Incidence trends and patterns of breast cancer in Sri Lanka: an analysis of the national cancer database," *BMC Cancer*, vol. 18, no. 1, 2018.
- [16] *Deep Learning* by Ian Goodfellow, Yoshua Bengio, and Aaron Courville published by MIT Press, 2016.
- [17] Stanford University's Course — CS231n: Convolutional Neural Network for Visual Recognition by Prof. Fei-Fei Li, Justin Johnson, Serena Yeung.
- [18] Y. Lecun, L. Bottou, Y. Bengio, and P. Haffner, "Gradient-based learning applied to document recognition," *Proc. IEEE Inst. Electr. Electron. Eng.*, vol. 86, no. 11, pp. 2278–2324, 1998.
- [19] A. Krizhevsky, I. Sutskever, and G. E. Hinton, "ImageNet classification with deep convolutional neural networks," *Commun. ACM*, vol. 60, no. 6, pp. 84–90, 2017.
- [20] H. Peiris, L. Mudduwa, N. Thalagala, and K. Jayatilake, "The value of Nottingham grade in breast cancer re-visited in the Sri Lankan setting," *Malays. J. Pathol.*, vol. 39, no. 2, pp. 141–148, 2017. 9
- [21] C. W. Elston and I. O. Ellis, "Pathological prognostic factors in breast cancer. I The value of histological grade in breast cancer: experience from a large study with long-term follow-up," *Histopathology*, vol. 19, no. 5, pp. 403–410, 1991.
- [22] A. Paul and D. P. Mukherjee, "Mitosis detection for invasive breast cancer grading in histopathological images," *IEEE Trans. Image Process.*, vol. 24, no. 11, pp. 4041–4054, 2015.
- [23] M. Talo, "Automated classification of histopathology images using transfer learning," *Artif. Intell. Med.*, vol. 101, no. 101743, p. 101743, 2019.
- [24] X. Wu, T. Yang, and Z. Xia, "Gait recognition based on DenseNet transfer learning," *Ijset.net*. [Online]. Available: <https://www.ijset.net/journal/2458.pdf>. [Accessed: 12-Jun-2021].
- [25] Q. Cai, X. Liu, and Z. Guo, "Identifying architectural distortion in mammogram images via a SE-DenseNet model and twice transfer learning," in *2018 11th International Congress on Image and Signal Processing, BioMedical Engineering and Informatics (CISP-BMEI)*, 2018.
- [26] S. Minaee, R. Kafieh, M. Sonka, S. Yazdani, and G. Jamalipour Soufi, "Deep-COVID: Predicting COVID-19 from chest X-ray images using deep transfer learning," *Med. Image Anal.*, vol. 65, no. 101794, p. 101794, 2020.
- [27] X. Xu, J. Lin, Y. Tao, and X. Wang, "An improved DenseNet method based on transfer learning for fundus medical images," in *2018 7th International Conference on Digital Home (ICDH)*, 2018.
- [28] Y. Celik, M. Talo, O. Yildirim, M. Karabatak, and U. R. Acharya, "Automated invasive ductal carcinoma detection based using deep transfer learning with whole-slide images," *Pattern Recognit. Lett.*, vol. 133, pp. 232–239, 2020.
- [29] F. Imrie, A. R. Bradley, M. van der Schaar, and C. M. Deane, "Protein family-specific models using deep neural networks and transfer learning improve virtual screening and highlight the need for more data," *J. Chem. Inf. Model.*, vol. 58, no. 11, pp. 2319–2330, 2018.
- [30] S. Pal and M. L. Gupta, "Correlation between cytological and histological grading of breast cancer and its role in prognosis," *J. Cytol.*, vol. 33, no. 4, pp. 182–186, 2016.
- [31] S.-H. Wang and Y.-D. Zhang, "DenseNet-201-based deep neural network with composite learning factor and precomputation for multiple sclerosis classification," *ACM trans. multimed. comput. commun. appl.*, vol. 16, no. 2s, pp. 1–19, 2020.
- [32] Y. Yari, T. V. Nguyen, and H. T. Nguyen, "Deep learning applied for histological diagnosis of breast cancer," *IEEE Access*, vol. 8, pp. 162432–162448, 2020.
- [33] A. Rakhlin, A. Shvets, V. Iglovikov, and A. A. Kalinin, "Deep convolutional neural networks for breast cancer histology image analysis," in *Lecture Notes in Computer Science*, Cham: Springer International Publishing, 2018, pp. 737–744.
- [34] "Breast cancer," *Uicc.org*. [Online]. Available: <https://www.uicc.org/what-we-do/thematic-areas-work/breast-cancer>. [Accessed: 12-Jun-2021]